



Image quality and dose reduction in cardiac interventional procedures: application of an optimization strategy with typical dose value analysis

 Assunção^{a,b}, M.F.M.;  Silva^c, J.O.;  Silva^b, G. C. C.;  Itikawa^{a,c}, E.N.

^a School of Electrical Mechanical and Computer Engineering – Federal University of Goiás, 74605-010, Goiânia, GO, Brazil.

^b CERRAD – Medical Physics and Radiation Protection Consultancy, 74810-033, Goiânia, GO, Brazil.

^c Institute of Physics – Federal University of Goiás, 74690-900, Goiânia, GO, Brazil.

*Correspondence: murillofelisberto@gmail.com

Abstract: This study aimed to evaluate the impact of dose-optimization strategies on radiation exposure during cardiac catheterization and angioplasty procedures. The investigation was carried out at a high-complexity referral center using retrospective data, clinical-protocol adjustments, and image-quality assessments with dedicated simulators. Implemented measures included reducing the cine dose per frame and enabling post-processing filters, resulting in reductions of up to 39 % in reference-point kerma and 25 % in noise intensity under low-dose conditions. In total, 714 procedures performed over five semesters were analyzed. Diagnostic reference levels (DRLs) were determined and compared with data from national and international literature. A statistically significant reduction in DAP (16.3 %) and $K_{a,r}$ (12.8 %) was observed for catheterization procedures ($p < 0.05$). Although angioplasty procedures showed a similar trend, case variability limited statistical significance. The results demonstrate the effectiveness of technical interventions and continuous monitoring in lowering exposure levels, without compromising diagnostic image quality.

Keywords: reference level; digital fluoroscopy; dose; image quality; optimization.



Qualidade de imagem e otimização da dose em cateterismo e angioplastia: efeitos da implementação e análise dos valores típicos de dose

Resumo: Este estudo teve como objetivo avaliar o impacto de estratégias de otimização de dose na exposição à radiação durante procedimentos de cateterismo e angioplastia cardíaca. A investigação foi conduzida em um centro de referência de alta complexidade, utilizando dados retrospectivos, ajustes em protocolos clínicos e avaliações da qualidade da imagem com simuladores dedicados. As medidas implementadas incluíram a redução da dose por quadro na cinefluoroscopia e a ativação de filtros de pós-processamento, resultando em reduções de até 39% na dose no ponto de referência e 25% na intensidade de ruído em condições de baixa dose. Ao todo, foram analisados 714 procedimentos realizados ao longo de cinco semestres. Níveis de referência diagnóstica (NRDs) foram determinados e comparados com dados da literatura nacional e internacional. Observou-se uma redução estatisticamente significativa no DAP (16,3%) e na dose no ponto de referência (12,8%) nos procedimentos de cateterismo ($p < 0,05$). Embora os procedimentos de angioplastia tenham apresentado tendência semelhante, a variabilidade dos casos limitou a significância estatística. Os resultados demonstram a eficácia das intervenções técnicas e do monitoramento contínuo na redução dos níveis de exposição, sem comprometer a qualidade da imagem diagnóstica.

Palavras-chave: nível de referência; fluoroscopia digital; dose; qualidade de imagem; otimização.

1. INTRODUCTION

Cardiovascular interventional radiology – particularly angiography and interventional cardiology – offers the major advantage of minimally invasive treatment, markedly lowering surgical risk compared with open cardiac surgery, thereby shortening patient recovery time and hospital stay [1]. Nevertheless, the ionizing radiation used to guide catheters and stents introduces additional, albeit generally low, risks that cannot be overlooked, especially during lengthy or complex procedures where adverse effects such as tissue damage have been documented [2][3].

In Brazil, cardiovascular interventional-radiology procedures such as angiography and angioplasty have become increasingly common, following international trends. A recent survey [4] indicates that about 125 926 angioplasties and 143 771 angiographies are performed annually, distributed across roughly 914 registered cath-labs nationwide [5]. This growth reflects both technological advances and the growing preference for less-invasive interventions.

Modern X-ray angiography systems incorporate advanced technological features – such as noise-reduction algorithms, contrast-optimization software and flexible pulse-rate control – that offer substantial scope for dose optimization [6]. Realizing this potential, however, demands that a multidisciplinary commissioning and quality-control team, including a medical physicist, verify how each manufacturer preset aligns with local clinical requirements; otherwise, default settings may inadvertently raise exposure. Effective optimization, therefore, combines equipment calibration with targeted tactics – tailored examination protocols, reduced pulse or frame rates, selective removal of anti-scatter grids, low-dose fluoroscopy modes and other advanced digital-processing options – while continuous staff training ensures that every technical adjustment is applied with a clear understanding of its impact on image quality and radiation burden. The practical influence

of these operational changes on patient and staff dose, as well as on image quality, is summarized in Table 1 [7].

Table 1: Impact of common fluoroscopic operating adjustments on image quality and on radiation dose to patients and staff; qualitative effects are indicated for each modification.

Operational change	Effect on image quality	Patient dose	Staff dose
Increase in patient size	Worse (higher scatter fraction)	Higher	Higher
Increase in tube current (mA) at constant tube voltage (KV) - AEC off	Better (lower noise)	Higher	Higher
Increase in tube voltage (KV) with AEC active	Soft tissue: better (lower noise); Bone & Iodine: lower contrast	Lower	Lower
Increase in source-to-skin distance	Slightly better	Lower	Little change
Increase in skin-to-detector distance	Slightly better (less scatter)	Higher	Higher
Increase in magnification factor	Better (higher spatial resolution)	Higher	Higher
Opening the collimator wider	Worse (higher scatter fraction)	Higher	Higher
Increase in exposure time	No effect	Higher	Higher
High-quality acquisition modes	Better (lower noise, higher resolution)	Higher	Higher

Source: [6].

The optimization process must be structured in five main steps: establishment of a quality-assurance programme; identification of the procedures that are priorities for initial optimization; modification of clinical protocols by the medical physicist; evaluation of the relationship between dose reduction and image quality; and implementation of a continuous training programme for the team involved. According to International Commission on Radiological Protection (ICRP 135), this structured approach ensures that the changes implemented have a measurable impact on clinical practice [8].

In this context, Diagnostic Reference Levels (DRLs) stand out as essential tools for dosimetry monitoring and the continuous evaluation of clinical practices. DRLs are reference values designed to control radiation exposure in medical examinations, ensuring doses within clinically acceptable standards. Defined as the third quartile of dose distributions obtained

from large samples of diagnostic centres – or as medians when only a few rooms are analyzed – DRLs function as an optimization tool, allowing the identification of excessive exposures without compromising diagnostic image quality [8].

In interventional radiology, dose-area product (DAP), fluoroscopy time, and number of images are commonly used to assess exposure practices [8]. These metrics are widely reported in the literature [9–27] and summarised in Table 2 across various centres, technologies, countries, and socioeconomic settings. The table focuses on the most frequent procedures in cardiac catheterisation labs: diagnostic coronary angiography (CA) and percutaneous transluminal coronary angioplasty (PTCA).

Table 2: Published national diagnostic reference levels (DRLs) for coronary catheterisation and angioplasty in various countries.

Qty. Of exams				CA		DRL PTCA	
Country	Centres	CA exams	PTCA exams	CA DAP (Gy.cm ²)	CA Time (min)	PTCA DAP (Gy.cm ²)	PTCA Time (min)
IAEA	-	2265	1844	50	9	125	22
Europe	9	672	662	45	6.5	85	15.5
England	110	18700		29	4.5	50	13
Ireland	14	967	597	41.74	5	83.56	17.8
Belgium	8	200	118	71.3	-	106	-
Croatia	4	138	151	32	6.6	72	19
United States	171	1326	672	83	5.4	193	18.5
Switzerland	23	311	319	102	15.49	125	30.6
Italy	5	103	79	49	4.87	100	16.9
Kenya	5	73	14	45.75	6.5	94	16
Greece	26	2572	1899	53	6	129	18
China	1	90	200	43.3	4.5	299	32.2
Australia	7	2590	947	58.65	-	129	-
South Korea	D	361	514	75.6	5.3	213	20.1
Qatar	3	-	-	72.14	4.67	143.7	8
France	61	48547	40026	38	6	80	15
Morocco	4	457	200	37.3	4.48	87.1	16.15
Spain	14	16631	136631	39	3.7	78	15
Brazil	6	907	921	94.6	-	88.6	-

Source: [9–27].

This study evaluated the performance of an angiographic system in cardiovascular interventions, analysing the impact of different configurations on radiation dose and image quality. It also compared the manufacturer's default settings with an optimised protocol, benchmarking patient dose results against published DRLs.

2. MATERIALS AND METHODS

The present study, approved by the local ethics committee (CAAE 84775618.1.0000.5505), was carried out in the Hemodynamics Department of Hospital São Francisco de Assis, a specialized referral centre for complex interventions in cardiology. Retrospective PACS data were used to determine the Typical Dose Values (TDVs), which informed subsequent dose monitoring and optimization strategies. All procedures were performed using a flat-panel angiographic system (Artis Zee Floor, Siemens Healthineers, Erlangen, Germany), installed in 2018, with custom adjustments to computational filters, current and voltage modulation, and image reconstruction algorithms via the system's "expert" mode, in partnership with the manufacturer.

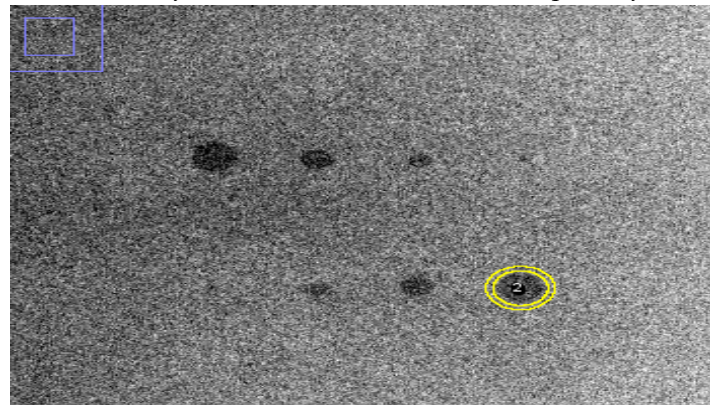
2.1. Image quality

Image quality was evaluated using dedicated simulators for hemodynamic procedures. A low-contrast phantom (Model MRA 07, MRA, São Carlos, Brazil), acquired in 2018, was employed. It contains circular structures with radii of 3.0 mm, 2.5 mm, 1.5 mm, and 0.5 mm, each with 1 % relative contrast, designed for assessing spatial and contrast resolution in fluoroscopic systems. Signal-to-noise ratio (SNR) was used as the primary metric, calculated as the ratio between the mean pixel value (MPV) and the standard deviation (σ) within the same region of interest (ROI), with σ representing image noise (Figure 1, Equation 1).

To assess the influence of exposure and image processing, images were acquired with dose levels ranging from 0.08 $\mu\text{Gy}/\text{frame}$ to 5.4 $\mu\text{Gy}/\text{frame}$, achieved by varying tube

current and pulse duration (Table 3). Each dose level was tested with all reconstruction kernels (Off, Normal, Smooth, and Sharp), allowing detailed analysis of noise and SNR across the full dynamic range for each algorithm. Quantitative analysis was performed using ImageJ (NIH, Bethesda, MD, USA) to extract signal and noise values within predefined ROIs. Table 3 summarizes the acquisition parameters and image processing modes used in the evaluation.

Figure 1: Regions of interest for SNR analysis in the MRA 07 phantom: central circular ROI for signal, surrounded by a 3 mm-radius ROI used to quantify noise.



Source: Authors.

$$SNR = \frac{MPV}{\sigma} \quad (1)$$

Table 3: Data acquired for image quality assessment at 70 kV tube voltage, 48 cm field size, and Single Shot mode. Each of the seven exposure levels was combined with all four reconstruction kernels (Off, Normal, Smooth, and Sharp), totaling 28 image sets.

Dose/ Frame ($\mu\text{Gy}/\text{frame}$)	Current (mA)	Time (ms)	Current-Time Product (mAs)
0.08	32.9	3.9	3.8
0.17	97.9	4.7	10.8
0.54	101.0	4.1	10.1
1.2	238.1	3.8	20.0
2.4	374.5	5.0	41.9
3.6	310.3	9.0	62.3
5.4	371.9	11.3	92.9

Source: Authors.

2.2. Determination of typical dose values

Dosimetric datasets were pulled from the Radiation Structured Dose Reports (RSDRs) that each examination automatically generates and stores in a dedicated directory. An R script (oro.dicom package) batch-exported, de-identified and tabulated the key fields: patient ID, operating physician, procedure type, reference-point kerma ($K_{a,r}$) (mGy), dose-area product ($\text{Gy} \cdot \text{cm}^2$) and fluoroscopy time (min).

For every six-month block, distributions of each quantity were analyzed: the median was adopted as the TDV, while quartiles and full data spread were recorded to flag outliers and temporal shifts. Results were presented to the interventional team twice a year to trigger protocol or technique adjustments. DAP was retained as the headline performance indicator because it is automatically logged, operator-independent and simultaneously reflects exposed area and dose level, facilitating comparisons across procedures and clinicians. [10]. Local TDVs were compared with regional, national and international reference-level studies to contextualize exposure levels and identify further optimization opportunities.

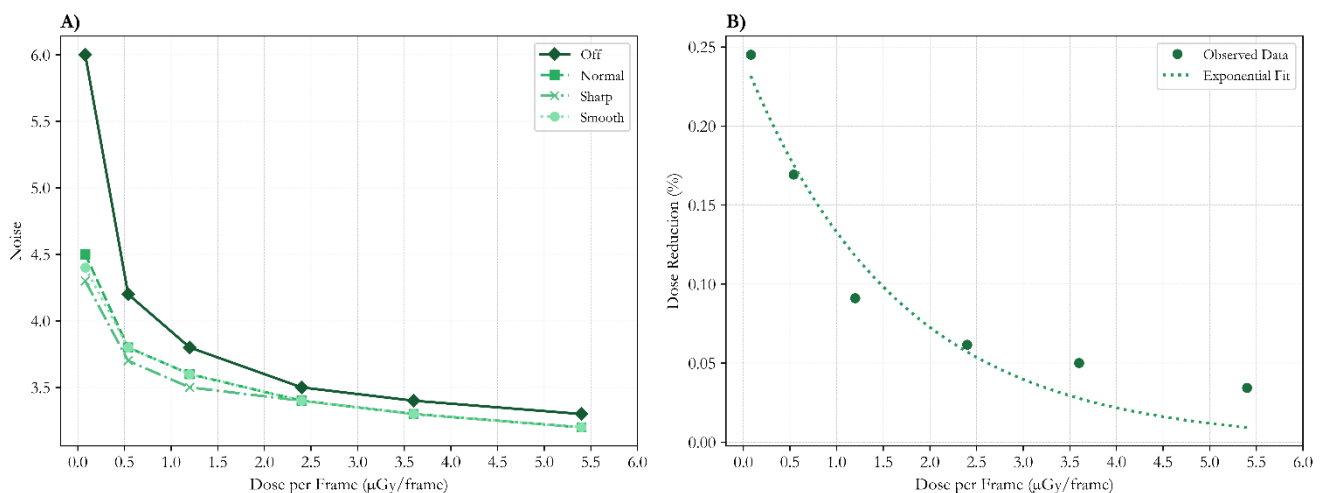
To compare data before and after the implementation of optimized protocols, the Mann-Whitney statistical test was applied to evaluate whether significant differences existed between the distributions of the analyzed populations. Statistical analysis was performed in Python, using the pandas and numpy packages to calculate medians and interquartile ranges (IQR), and scipy.stats for hypothesis testing. Continuous variables were assessed for distribution and, as they were non-normal, are expressed as medians and IQR. A significance level of $p < 0.05$ was adopted for all comparisons.

3. RESULTS

3.1. Noise characterization

Noise behavior in the detector was assessed from post-processed images, since it was not possible to obtain files in the “for processing” format. The performance curves used for optimization were based on the data shown in Figure 2, which displays the noise measured in the 3 mm structure of the low-contrast MR-07 simulator. The SNR metric was applied as described in Equation 1. Similar behavior was observed among the kernels evaluated at different exposure levels. However, a significant difference was identified when processing was activated, particularly under low-exposure conditions. It is also important to note that increasing the dose per frame at the detector level will proportionally increase entrance skin dose in high-attenuation patients, such as those with obesity.

Figure 2: Noise measured in the 3 mm-radius insert across the tested dose range. A) Detector noise versus dose per frame for each reconstruction kernel (Off, Normal, Sharp, Smooth). B) Percentage noise reduction for the Normal kernel relative to Off at the same dose levels.



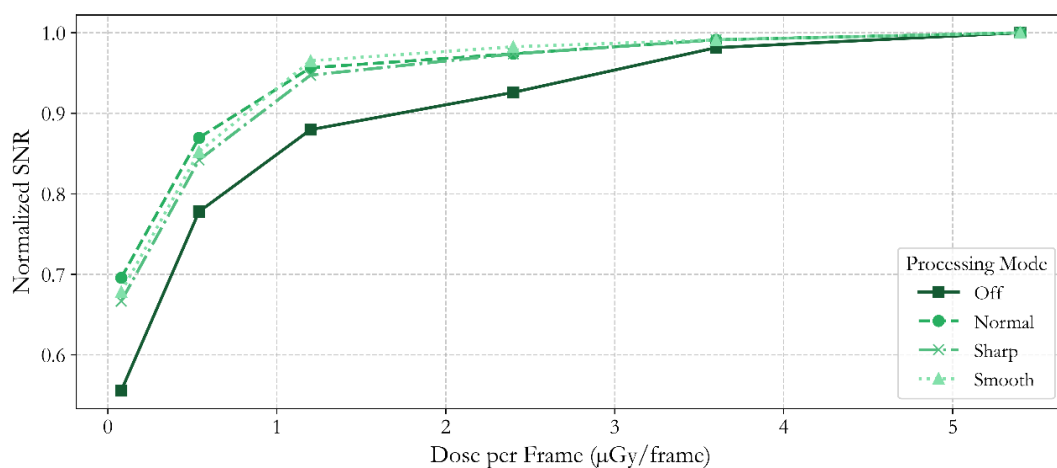
Source: Authors.

As illustrated in Figure 3, increasing the exposure parameter led to a gradual reduction in the noise difference between processed and unprocessed images. The noise ratio between the *Normal* and *Off* kernels dropped to 3.4 %, while exposures below 1.2 μGy/frame achieved up to 25 % noise reduction. Above 1.82 μGy/frame, noise levels stabilized, indicating the limited effect of filtering at higher exposures. These findings suggest that smoothing filters

are most effective under low-dose conditions, whether due to reduced acquisition settings or clinical scenarios involving greater attenuation, such as in obese patients. To address the expected increase in image noise following dose reduction, the smoothing filter was applied in the “Normal” mode.

The SNR curve, also shown in Figure 3 and normalized to the maximum value at 5.2 $\mu\text{Gy}/\text{frame}$, demonstrates that approximately 95 % of the peak SNR is already reached at 1.82 $\mu\text{Gy}/\text{frame}$. Below this point, the curve declines more sharply, indicating a steeper loss in image quality. Beyond 2.0 $\mu\text{Gy}/\text{frame}$, the SNR levels off, confirming that further dose increases offer no meaningful improvement in image performance.

Figure 3: Normalised SNR versus dose per frame for each reconstruction kernel measured in the 3 mm-radius insert; $\approx 95\%$ of peak SNR is reached at 1.82 $\mu\text{Gy}/\text{frame}$, with minimal gain at higher doses.



Source: Authors.

3.2. Optimization proposal

Based on image quality analysis, an optimization strategy was implemented to reduce the cine dose per frame from 3.00 - 1.82 μGy – a 39 % decrease in reference point kerma – with an estimated 17 % increase in image noise. To offset this, the “normal” smoothing kernel was applied, reducing noise by 9.7 %. Importantly, none of the four clinical teams reported any loss in diagnostic quality after implementation. Table 4 lists the revised exposure parameters, while Table 5 details the study population and procedure distribution, providing context for the comparison between standard and optimized protocols.

Table 4: Key cine-fluoroscopy settings before and after protocol optimisation.

Parameter	Optimized	Standard
Tube voltage (KV)	70	70
Maximum tube voltage (KV)	96	96
Pulse width (ms)	80	80
Detector dose ($\mu\text{Gy}/\text{frame}$)	1,82	3
Processing type	DSA	DSA
Pulse rate (frames/s)	3	3
i-Noise-reduction processing	Normal	OFF

Table 5: Patient demographics and CA/PTCA counts under standard versus optimised protocols.

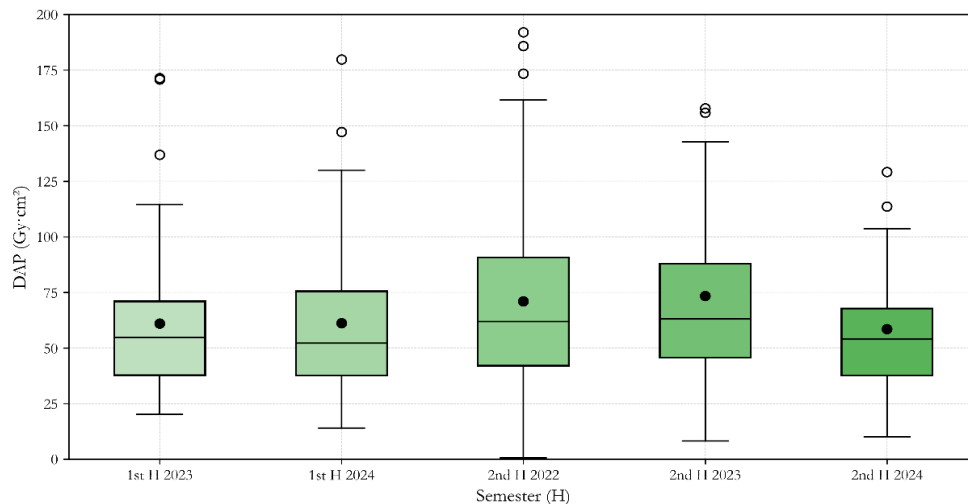
Parameter	Value
Age (years)	64.7 (22 - 93)
BMI (Kg/m^2)	27.3 (17.9 - 44.6)
Male sex (%)	58.3
Female sex (%)	41.7
Total procedures	1306
Parameter	CAPTCA
Total	473 275
Standard protocol	170 96
Optimized protocol	298 143

3.3. Characterization of exposure levels – cardiac catheterization

To assess typical dose and fluoroscopy time levels in catheterization procedures, a total of 473 examinations were analyzed. The exposure results are presented in Figure 4, which illustrates the distribution of DAP values. Notable fluctuations are observed across the dataset, with a clear shift following protocol optimization. In the second half of 2022, the median DAP was approximately $63.05 \text{ Gy}\cdot\text{cm}^2$. Following the introduction of systematic dose recording and technical adjustments, this median decreased to $53.9 \text{ Gy}\cdot\text{cm}^2$ in the second half of 2024, a reduction of about 14.5 %. A simultaneous decrease in the interquartile range (Q3–Q1) and in the number of outliers suggests increased consistency in exposure levels and greater standardization of clinical practice.

Although the reduction may be associated with changes in cine mode or new clinical routines, ongoing monitoring remains essential to ensure that dose levels stay within acceptable limits. In July and August 2024, a reset of the equipment protocols temporarily reversed some of the optimization measures, resulting in a transient rise in DAP to values similar to those recorded in the second half of 2023. After protocol readjustments were reapplied, exposure levels returned to values close to those observed in the first half of 2023.

Figure 4: Box-plot of DAP values for coronary catheterisation procedures by semester; dots indicate the medians, used here as the typical dose values.



Source: Authors.

As shown in Figure 5, analysis of the facility's DAP levels over time reveals that typical values remain consistently above the reference level proposed by the IAEA ($50 \text{ Gy}\cdot\text{cm}^2$). In comparison, countries with established regional dose management systems, such as Spain ($39 \text{ Gy}\cdot\text{cm}^2$; $n = 88\,573$) and France ($38 \text{ Gy}\cdot\text{cm}^2$; $n = 153\,262$), report significantly lower median values. England, with a national median of $29 \text{ Gy}\cdot\text{cm}^2$, presents even more substantial reductions, highlighting the impact of coordinated national monitoring initiatives on dose optimization. The most recent median value recorded at the facility – $54 \text{ Gy}\cdot\text{cm}^2$ – exceeds 63.16 % of the values reported in the literature, suggesting that while progress has been made, further improvements in dose management are still warranted.

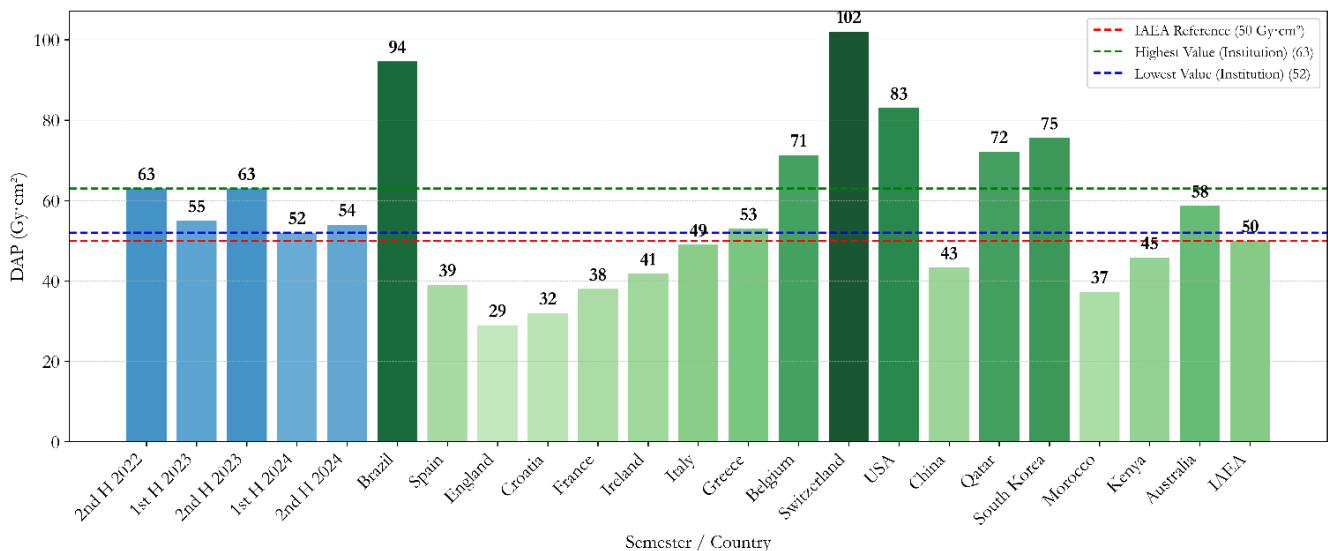
Table 6: DAP, reference-point air kerma ($K_{a,r}$) and fluoroscopy time for coronary catheterisation under the standard and optimised protocols; values are presented as mean \pm SD and as quartiles.

Period	DAP($\text{Gy}\cdot\text{cm}^2$)				$K_{a,r}$ (mGy)				Tempo (min)			
	Mean \pm SD	Q1	Median	Q3	Mean \pm SD	Q1	Median	Q3	Mean \pm SD	Q1	Median	Q3
Standard	76 ± 75	44	62	88	872 ± 670	553.6	756	1041	7.0 ± 8.7	3	4.7	7.6
Optimized	60 ± 37	37	52	71	730 ± 425	470.8	659	889	5.7 ± 5.1	3	4.1	6.9

Source: Authors.

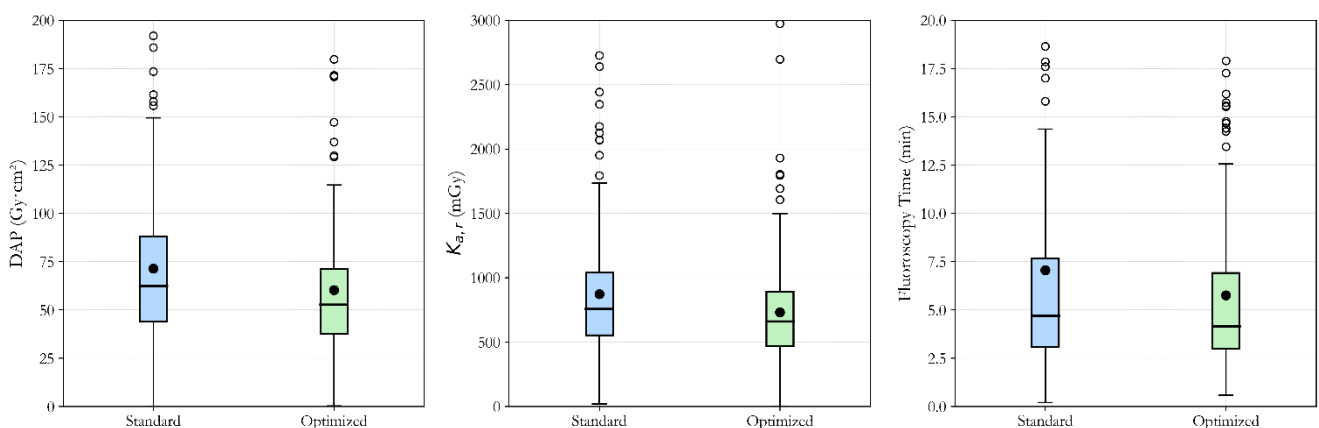
The impact of protocol optimization is illustrated in Figure 6, which compares the standard and optimized protocols through side-by-side box-plots and shows that optimization significantly lowered patient dose: the median DAP fell 16.3 % ($62.87 \rightarrow 52.67 \text{ Gy} \cdot \text{cm}^2$) and the median $K_{a,r}$ dropped 12.8 % ($756.6 \rightarrow 659.5 \text{ mGy}$), both with $p < 0.05$ in the Mann-Whitney test. The accompanying shrinkage of the interquartile ranges signals more consistent practice. Fluoroscopy time declined only marginally – from 21.4 to 20.1 min – and this change was not statistically significant ($p = 0.05$), indicating that operator-related variability persists.

Figure 5: Typical dose values for coronary catheterisation compared with international studies; dashed lines indicate the IAEA reference level and this study's highest and lowest TVDs.



Source: Authors.

Figure 6: Combined catheterisation dataset comparing standard and optimised protocols: box-plots of DAP ($\text{Gy} \cdot \text{cm}^2$), reference-point air kerma $K_{a,r}$ (mGy) and fluoroscopy time (min).



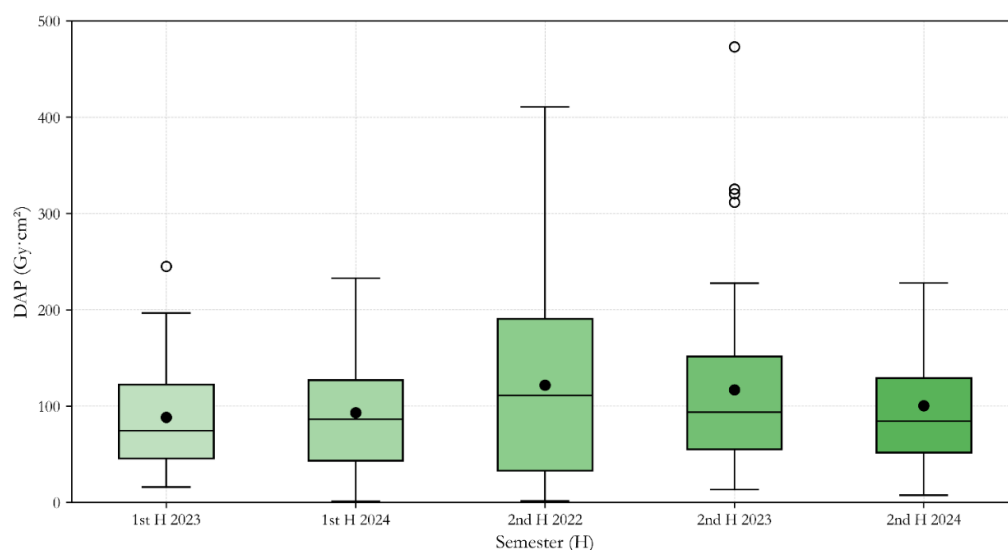
Source: Authors.

3.4. Characterization of exposure levels – cardiac angioplasty

As with catheterization procedures, typical dose and fluoroscopy-time levels in cardiac angioplasty were assessed to evaluate the impact of optimization strategies. A total of 298 examinations were analyzed, with the DAP distribution presented in Figure 7. Relevant variations were observed across the periods, with significant changes following the implementation of protocol adjustments. In the second half of 2022, the median DAP was approximately $111.14 \text{ Gy}\cdot\text{cm}^2$. After systematic dose recording and the introducing of technical changes, this value dropped to $74.59 \text{ Gy}\cdot\text{cm}^2$ in the first half of 2023. In subsequent periods, the median fluctuated slightly, reaching $84.38 \text{ Gy}\cdot\text{cm}^2$ in the second half of 2024 – representing an overall reduction of around 24 % compared to the initial value.

This reduction reflects a positive response to the optimization interventions adopted. However, the fluctuations observed in the later semesters highlight the need for continuous monitoring to ensure the sustained effectiveness of these strategies. As also seen in the catheterization data, a notable decrease in data dispersion was identified from the second half of 2023 onward, indicating greater consistency in DAP values and improved standardization of clinical practice

Figure 7: Box-plot of DAP values for coronary angioplasty procedures by semester; dots mark the medians, used here as the typical dose values.



Source: Authors.

As presented in Figure 8, DAP values for angioplasty remained consistently below the IAEA reference level of $125 \text{ Gy}\cdot\text{cm}^2$ across all semesters. However, when compared to countries with established national dose-monitoring programmes, such as England ($50 \text{ Gy}\cdot\text{cm}^2$) and France ($80 \text{ Gy}\cdot\text{cm}^2$), the facility's values are still higher. These findings, consistent with the patterns previously discussed for catheterization, reflect the influence of structured dose management on reducing exposures, as noted by Aly *et al.* (2021). The most recent median ($84 \text{ Gy}\cdot\text{cm}^2$) is higher than only 24 % of the international reference values, indicating that although local exposure levels are within acceptable ranges, further optimization is both possible and desirable.

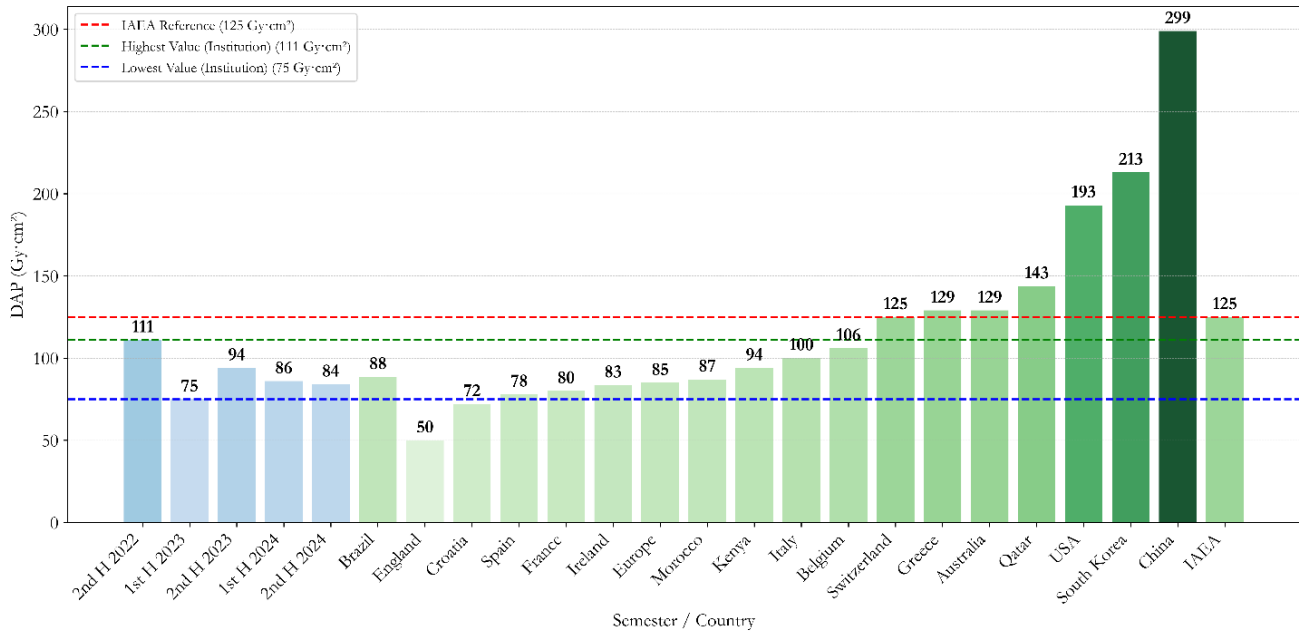
Table 7 summarizes angioplasty exposure metrics for the standard protocol and the optimized protocol, presenting mean \pm SD alongside the median and interquartile range (Q1–Q3) for DAP, $K_{a,r}$ and fluoroscopy time.

Table 7: DAP, reference-point air kerma ($K_{a,r}$) and fluoroscopy time for coronary angioplasty under the standard and optimised protocols; values are presented as mean \pm SD and as quartiles (Q1, median, Q3).

	DAP($\text{Gy}\cdot\text{cm}^2$)				$K_{a,r}$ (mGy)				Time (min)			
	Mean \pm SD	Q1	Median	Q3	Mean \pm SD	Q1	Median	Q3	Mean \pm SD	Q1	Median	Q3
Standard	116 ± 93	49	94	167	1628 ± 1387	577	1209	2315	18.2 ± 22.2	6.9	11.8	24.7
Optimized	93 ± 71	46	81	127	1628 ± 1233	569	963	1700	13.2 ± 10	5.7	10.7	16.8

Source: Authors.

Figure 8: Typical dose values (TVD) for coronary angioplasty compared with international studies; dashed lines indicate the IAEA reference level and this study's highest and lowest TVDs.



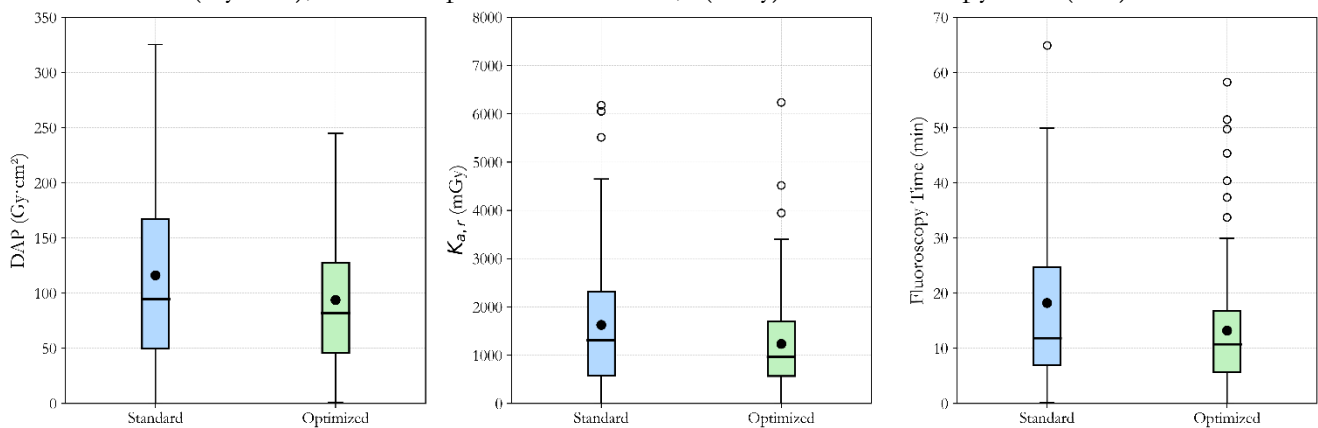
Source: Authors.

Similarly, to what was observed in catheterization, the switch to the optimized protocol lowered typical values: median DAP dropped 18.6 % ($116.15 \rightarrow 94.43 \text{ Gy} \cdot \text{cm}^2$), median dose 12.8 % ($963 \rightarrow 841 \text{ mGy}$) and median fluoroscopy time 9 % ($11.85 \rightarrow 10.73 \text{ min}$); overall means fell by 24.3 %, 28.8 % and 20 %, respectively. Interquartile ranges also narrowed, indicating more consistent technique.

Figure 9 illustrates these results with a side-by-side box-plot of the two populations; a Mann-Whitney test performed on the same data ($\alpha = 0.05$) yielded p-values > 0.05 for both DAP and $K_{a,r}$, and likewise for fluoroscopy time, reflecting the high intrinsic variability of angioplasty. This variability may be attributed to several factors, including the diversity of operators involved, the range of procedural complexity (diagnostic vs therapeutic cases), and reconfigurations made to the system during the optimisation period. Additionally, our equipment does not allow automatic separation of combined procedures (angioplasty + catheterization) from isolated angioplasties, which further increases the heterogeneity of the dataset and may have limited statistical significance despite the observed trends. Despite the

lack of statistical significance, the concurrent reductions in central tendency and dispersion confirm a positive trend toward dose optimization and practice stabilization.

Figure 9: Combined angioplasty dataset comparing standard and optimised protocols: box-plots of DAP ($\text{Gy}\cdot\text{cm}^2$), reference-point air kerma $K_{a,r}$ (mGy) and fluoroscopy time (min).



Source: Authors.

4. CONCLUSIONS

This study demonstrates that optimization strategies in cardiac catheterization and angioplasty procedures led to meaningful reductions in radiation exposure without compromising diagnostic quality. In catheterization, statistically significant decreases were observed in both DAP and $K_{a,r}$, while angioplasty showed consistent downward trends despite greater variability. Measures such as lowering the cine dose per frame and applying image filters proved effective in reducing dose, with experimental data confirming improved image uniformity and SNR. These findings reinforce the value of targeted technical adjustments as part of a broader optimization strategy.

The findings of this study highlight the importance of maintaining continuous optimization efforts in interventional cardiology. Strengthening a culture of radiation protection through protocol standardization, systematic monitoring and multidisciplinary collaboration is essential to ensure consistent improvements in clinical practice. The typical dose values obtained in this study will support future multicenter efforts to define local

DRLs, helping to address the current lack of consolidated national data. This work contributes to that broader effort, offering a foundation for future regulatory developments, quality assurance programmes and public policies focused on radiological safety in interventional procedures.

ACKNOWLEDGMENT

The authors thank Hospital São Francisco de Assis for providing access to the hemodynamics department and for the cooperation of the technical and clinical teams during the conduct of the study. We also acknowledge the financial support of the Brazilian Coordination for the Improvement of Higher Education Personnel (CAPES) through a scholarship grant.

CONFLICT OF INTEREST

All authors declare that they have no conflicts of interest.

REFERENCES

- [1] EUCLID CONSORTIUM. Radiation dose and diagnostic reference levels for four interventional radiology procedures: results of the prospective European multicenter survey EUCLID. **European Radiology**, 2023.
- [2] GUESNIER-DOPAGNE, Mélanie et al. Incidence of chronic radiodermatitis after fluoroscopically guided interventions: a retrospective study. **Journal of Vascular and Interventional Radiology**, v. 30, n. 5, p. 692-698. e13, 2019.
- [3] CHENG, Ting Ting; YANG, Hui-Ju. Chronic radiation dermatitis induced by cardiac catheterization: a case report and literature review. **Acta Dermatovenereologica Alpina, Pannonica, et Adriatica**, v. 31, n. 4, p. 147-149, 2022.

- [4] OLIVEIRA, G. M. M. *et al.* Estatística Cardiovascular – Brasil 2020. **Arquivos Brasileiros de Cardiologia**, v. 115, n. 3, p. 308-439, 2020.
- [5] FRANCISCO, M. F. F. **Avaliação da disponibilidade e acesso aos equipamentos de hemodinâmica no Brasil**. Dissertação (Mestrado em Ciências) – Universidade Federal de São Paulo, São Paulo, 2021.
- [6] TSALAFOUTAS, I. A.; TSAPAKI, V.; TRIANTOPOULOU, I. Evaluation of image quality and patient exposure in fluoroscopy using a phantom: is there any clinical relevance? **European Journal of Radiology**, v. 138, p. 109607, 2021.
- [7] BUSHBERG, J. T.; SEIBERT, J. A. **The essential physics of medical imaging study guide**. s.l.: Lippincott Williams & Wilkins, 2022.
- [8] TSAPAKI, V. Radiation dose optimization in diagnostic and interventional radiology: current issues and future perspectives. **Physica Medica**, v. 79, p. 16-21, 2020.
- [9] VAÑÓ, E. *et al.* ICRP publication 135: diagnostic reference levels in medical imaging. **Annals of the ICRP**, v. 46, n. 1, p. 1-144, 2017.
- [10] INTERNATIONAL ATOMIC ENERGY AGENCY. Establishing guidance levels in X-ray guided medical interventional procedures. Vienna: IAEA, 2009.
- [11] HART, D.; HILLIER, M. C.; WALL, B. F. *et al.* National reference doses for common radiographic, fluoroscopic and dental X-ray examinations in the UK. **British Journal of Radiology**, London, v. 82, n. 973, p. 1-12, 2009.
- [12] PADOVANI, R.; COMPAGNONE, G.; D'ERCOLE, L.; *et al.* Livelli diagnostici di riferimento nazionali per la radiologia diagnostica e interventistica. **Rapport ISTISAN**, Rome, n. 17/33, 2017.
- [13] BOGAERT, E.; BACHER, K.; THIERENS, H. A large-scale multicentre study in Belgium of dose area product values and effective doses in interventional cardiology using contemporary X-ray equipment. **Radiation Protection Dosimetry**, Oxford, v. 128, n. 3, p. 312-323, 2008.
- [14] D'HELT, C. J.; BRENNAN, P. C.; MCGEE, A. M. *et al.* Potential Irish dose reference levels for cardiac interventional examinations. **British Journal of Radiology**, v. 82, n. 976, p. 296-302, 2009.
- [15] BRNIĆ, Z.; KRPAN, T.; FAJ, D. *et al.* Patient radiation doses in the most common interventional cardiology procedures in Croatia: first results. **Radiation Protection Dosimetry**, v. 138, n. 2, p. 180-186, 2009.

- [16] MILLER, D. L.; HILOHI, C. M.; SPELIC, D. C. *et al.* Patient radiation doses in interventional cardiology in the US: advisory data sets and possible initial values for US reference levels. **Medical Physics**, v. 39, n. 10, p. 6276-6286, 2012.
- [17] SAMARA, E. T.; AROUA, A.; DE PALMA, R. *et al.* An audit of diagnostic reference levels in interventional cardiology and radiology: are there differences between academic and non-academic centres? **Radiation Protection Dosimetry**, v. 148, n. 1, p. 74-82, 2011.
- [18] COMPAGNONE, G.; CAMPANELLA, F.; DOMENICHELLI, S. *et al.* Survey of interventional cardiology procedures in Italy. **Radiation Protection Dosimetry**, v. 150, n. 3, p. 316-324, 2012.
- [19] KORIR, G. K.; WAMBANI, J. S.; YUKO-JOWI, C. A. *et al.* Establishing diagnostic reference levels for interventional procedures in Kenya. **Radiography**, v. 20, n. 2, p. 148-152, 2014.
- [20] SIMANTIRAKIS, G.; KOUKORAVA, C.; KALATHAKI, M.; *et al.* Reference levels and patient doses in interventional cardiology procedures in Greece. **European Radiology**, v. 23, n. 8, p. 2324-2332, 2013.
- [21] CUI, Y.; ZHANG, H.; ZHENG, J.; YANG, X.; LIANG, C. An investigation of patient doses during coronary interventional procedures in China. **Radiation Protection Dosimetry**, v. 156, n. 3, p. 296-302, 2013.
- [22] CROWHURST, J. A. *et al.* Radiation dose in coronary angiography and intervention: initial results from the establishment of a multi-centre diagnostic reference level in Queensland public hospitals. **Journal of Medical Radiation Sciences**, v. 61, n. 3, p. 135-141, 2014.
- [23] KIM, J.; SEO, D.; CHOI, I. *et al.* Development of diagnostic reference levels using a real-time radiation dose monitoring system at a cardiovascular center in Korea. **Journal of Digital Imaging**, v. 28, n. 6, p. 684-694, 2015.
- [24] ALY, A. E.; DUHAINI, I. M.; MANAA, S. M. *et al.* Patient peak skin dose and dose area product from interventional cardiology procedures. **International Journal of Medical Physics, Clinical Engineering and Radiation Oncology**, v. 4, n. 1, 2015.
- [25] GEORGES, J. L.; BELLE, L.; ETARD, C. *et al.* Radiation doses to patients in interventional coronary procedures: estimation of updated national reference levels by dose audit. **Radiation Protection Dosimetry**, v. 175, n. 1, p. 17-25, 2016.

- [26] OU-SAADA, I. *et al.* Local diagnostic reference levels in interventional radiology. **Journal of Medical Imaging and Radiation Sciences**, v. 51, n. 2, p. 307-311, 2020.
- [27] VIEIRA, L. A. *et al.* Diagnostic Reference Levels Based on Patient Body Mass Index for Select Interventional Procedures in Minas Gerais/Brazil. **Radiation Protection Dosimetry**, v. 198, n. 7, p. 379-385, 2022.

LICENSE

This article is licensed under a Creative Commons Attribution 4.0 International License, which permits use, sharing, adaptation, distribution and reproduction in any medium or format, as long as you give appropriate credit to the original author(s) and the source, provide a link to the Creative Commons license, and indicate if changes were made. The images or other third-party material in this article are included in the article's Creative Commons license, unless indicated otherwise in a credit line to the material.

To view a copy of this license, visit <http://creativecommons.org/licenses/by/4.0/>.